

Supplementary Information

Mechanochromic Luminescence in Copper Nanoclusters: Resolving Structural Transitions through Microcrystal Electron Diffraction

*Harshita Nagar^ξ, Subrata Duary^ξ, Vivek Yadav^ξ, Amoghavarsha Ramachandra Kini^ξ, Sudhadevi Antharjanam^φ, Tomas Base^{*ψ}, Anirban Som^{*ξ}, Brent L. Nannenga^{*€}, and Thalappil Pradeep^{*ξ}*

^ξ DST Unit of Nanoscience (DST UNS) and Thematic Unit of Excellence (TUE), Department of Chemistry, Indian Institute of Technology, Madras, Chennai – 600036, International Centre for Clean Water, Chennai- 600113, India

[€] School of Engineering of Matter, Transport and Energy, Arizona State University, Tempe, Arizona, United States

^φ Sophisticated Analytical Instruments Facility (SAIF), Indian Institute of Technology, Madras, Chennai – 600036, India

^ψ Department of Synthesis, Institute of Inorganic Chemistry, The Czech Academy of Science, 1001 Husinec-Rez, 25068, Czech Republic

* Email: pradeep@iitm.ac.in, brent.nannenga@asu.edu, asomchem@gmail.com, tbase@iic.acs.cz

Table of contents:

Sl No.	Contents	Page No.
1.	Experimental section	3
2.	Instrumentation	4
3.	Characterization	5
Fig S1.	UV-vis absorption spectra and ESI-MS of Cu ₄ (MNA) ₂ (DPPE) ₂ , Cu ₄ (<i>o</i> ₉ -CBT) ₄ and Cu ₄ (<i>m</i> ₉ -CBT) ₄	6
Fig S2.	MicroED sample preparation and data collection workflow	6
Fig S3.	MicroED data acquisition workflow	7
Fig S4.	TEM images (Images of crystal taken at different tilts from -50° to 50°)	7
Table S1.	Comparison of unit cell parameters, space group, bond lengths (Å), bond angles (°), and structure refinement details of Cu ₄ (MNA) ₂ (DPPE) ₂ obtained from SC-XRD and MicroED	8
Fig S5.	Unit cell molecular packing of MicroED structure of	9

	Cu ₄ (MNA) ₂ (DPPE) ₂	
Fig S6.	Single crystal X-ray structure of Cu ₄ (MNA) ₂ (DPPE) ₂	9
Table S2.	Comparison of unit cell parameters, space group, bond lengths (Å), bond angles (°), and structure refinement details of Cu ₄ (<i>m</i> ₉ -CBT) ₄ obtained from SC-XRD and MicroED	10
Fig S7.	Single crystal X-ray structure of Cu ₄ (<i>m</i> ₉ -CBT) ₄	11
Fig S8.	Unit cell packing of MicroED structure of Cu ₄ (<i>m</i> ₉ -CBT) ₄	11
Table S3.	Comparison of unit cell parameters, space group, bond lengths (Å), bond angles (°), and structure refinement details of Cu ₄ (<i>o</i> ₉ -CBT) ₄ obtained from SC-XRD and MicroED in the initial crystalline state and after restoration of crystallinity upon solvent vapor exposure	12
Fig S9.	Single crystal X-ray structure of Cu ₄ (<i>o</i> ₉ -CBT) ₄	13
Fig S10.	Unit cell packing of MicroED structure of Cu ₄ (<i>o</i> ₉ -CBT) ₄	13
Table S4.	Crystallographic information of Cu ₄ (MNA) ₂ (DPPE) ₂	14
Table S5.	Crystallographic information of Cu ₄ (<i>o</i> ₉ -CBT) ₄	15
Table S6.	Crystallographic information of Cu ₄ (<i>m</i> ₉ -CBT) ₄	16
Table S7.	Atomic coordinates of Cu ₄ (MNA) ₂ (DPPE) ₂ crystal	17
Table S8.	Atomic coordinates of Cu ₄ (<i>o</i> ₉ -CBT) ₄ crystal in initial state (before grinding)	20
Table S9.	Atomic coordinates of Cu ₄ (<i>o</i> ₉ -CBT) ₄ crystal after solvent vapor exposure	21
Table S10.	Atomic coordinates of Cu ₄ (<i>m</i> ₉ -CBT) ₄ crystal	22
	References	24

1. Experimental section

Chemicals

Copper iodide (CuI), 1,2-bis-diphenylphosphino ethane (DPPE), 2-mercaptopicotonic acid (MNA), and sodium borohydride (NaBH_4) were purchased from Aldrich Chemicals. ortho-carborane-9-thiol ($o_9\text{-CBT}$), and meta-carborane-9-thiol ($m_9\text{-CBT}$) were synthesized according to the reported procedure^{1,2}. Solvents used were acetonitrile, methanol, acetone, toluene, dichloromethane, N,N-dimethylformamide, and n-hexane purchased from Rankem and Finar India.

Nanoclusters synthesis

All three Cu_4 nanoclusters were synthesized using previously reported method^{3,4} with modifications where the LEIST method in $[\text{Cu}_{18}\text{H}_{16}(\text{DPPE})]^{2+}$ nanocluster was used.

Synthesis of Cu_{18} NC – Cu_{18} NC was synthesized using a previously available procedure⁵. 95 mg of CuI with 120 mg DPPE was added in 15 ml acetonitrile. Then reduction is carried out using 180 mg of reducing agent i.e., NaBH_4 . After 4 hrs of stirring, an orange colour precipitate was obtained which was cleaned three times using methanol and acetonitrile then Cu_{18} was extracted in DCM.

- a) **Synthesis of $\text{Cu}_4(\text{MNA})_2(\text{DPPE})_2$ NC** - The Cu_4 nanoclusters were synthesized through Ligand Exchange-Induced Structural Transformation (LEIST) method using Cu_{18} as the precursor. Approximately 35 mg of purified Cu_{18} , dissolved in 4 mL of dichloromethane (DCM), was reacted with 15 mg of 2-mercaptopicotinic acid in 1 mL of dimethylformamide (DMF). The initial reaction mixture appeared transparent and reddish. After 45 minutes, the solution turned yellowish, indicating the progression of reaction, and then the reaction was stopped.
- b) **Synthesis of $\text{Cu}_4(o_9\text{-CBT})_4$ NC** – This cluster was formed using the above synthesized Cu_{18} NC using (LEIST) where 50 mg Cu_{18} in DCM was mixed with 35 mg ortho carborane-9-thiol ligand and kept for stirring at room temperature. After 3 hrs, the solution, initially yellow in color forms white precipitates. These white precipitates shows green emission under 365 nm UV lamp. The reaction was allowed to continue for 5 hrs until completion. The resulting microcrystalline white precipitates were thoroughly washed with methanol and DCM to remove any excess unreacted ligands. These white precipitates were soluble in acetone and further purified through crystallization.

c) **Synthesis of Cu₄(m₉-CBT)₄ NC** – Cu₄(m-CBT)₄ NC was formed using the same procedure used for Cu₄(o-CBT)₄ NC but this time ligand used was meta carborane – 9 -thiol. The as formed cluster was soluble in DCM. The reaction solvents were removed using rotavapor, and the solid white product that formed showed a green luminescence under a 365 nm UV lamp.

Crystallization

Cu₄(MNA)₂(DPPE)₂ was crystallized through hexane vapor diffusion, resulting in a crude yellow solution at 4 °C³.

Cu₄(o₉-CBT)₄ – acetone solution of Cu₄(o₉-CBT)₄ was mixed with equal amount of dichloromethane and kept for crystallization at 4°C. Large hexagonal crystals formed after a week⁴.

Cu₄(m₉-CBT)₄ – dichloromethane solution of Cu₄(m₉-CBT)₄ was mixed with equal amount of toluene and kept for crystallization at 4°C. Large parallelepiped crystals formed after a week⁴.

2. Instrumentation

UV-vis spectroscopy

UV-vis absorption spectra were recorded over a wavelength range of 1100–200 nm using a Perkin Elmer Lambda 365 UV-vis spectrometer equipped with a 1 nm bandpass filter. The spectra were acquired at a scan rate of 100 nm/min.

Mass spectrometry

Mass spectra of these three nanoclusters were obtained using a Waters Synapt G2Si HDMS instrument. For Cu₄(MNA)₂(DPPE)₂ NC, conditions used were capillary voltage - 3kV, flow rate – 20 µL/min, source temperature – 100° C, desolvation temperature – 150° C and gas flow rate – 400 L/h. In case of Cu₄(o₉-CBT)₄ and Cu₄(m₉-CBT)₄, formic acid and cesium acetate respectively were used as ionization enhancer. Conditions used were capillary voltage – 3kV, cone voltage – 0kV, source temperature – 50° C, desolvation temperature – 90° C and gas flow rate – 300L/h.

TEM

TEM imaging of the microcrystals was performed on a ThermoScientific Krios G4 transmission electron microscope operated at an accelerating voltage of 300 kV. Samples were

prepared by depositing microcrystals onto lacey carbon grids. Images were acquired using a Ceta D CMOS camera under low electron dose conditions (spot size 8) to minimize beam-induced damage and preserve structural integrity. This approach ensured high-contrast visualization of the microcrystalline morphology while maintaining sample quality for subsequent MicroED data collection.

3. Characterization

UV-vis. absorption spectra - The UV-vis optical absorption spectrum of Cu₄(MNA)₂(DPPE)₂ NC in acetonitrile displays distinct peaks at 297 nm and 380 nm. Also, the UV-vis optical absorption spectra of Cu₄(*o*₉-CBT)₄ and Cu₄(*m*₉-CBT)₄ in acetonitrile exhibit single absorption bands at 281 nm and 279 nm, respectively.

Mass spectrometry - The Cu₄(MNA)₂(DPPE)₂ NC was ionized in positive ion mode, exhibiting a characteristic peak at m/z 1357.95 (1+), corresponding to [Cu₄(MNA)₂(DPPE)₂]⁺. The experimental isotopic distribution matches the theoretical isotopic distribution (inset left). Additional, prominent mass peaks observed at m/z 1380.90 (1+), 1396.94 (1+), and 1434.92 (1+), denoted as i, ii, and iii, respectively, are attributed to sodium and potassium species attached to the molecular ion of the cluster. When Cu₄(*o*₉-CBT)₄ and Cu₄(*m*₉-CBT)₄ were characterized by ESI-MS, no characteristic peaks were detected from the as-prepared samples in either positive or negative ion modes, indicating that the clusters are neutral. However, in the presence of formic acid, Cu₄(*o*₉-CBT)₄ exhibited a characteristic peak at m/z 956.7, suggesting that protonation facilitated the ionization of the cluster. Similarly, in the presence of cesium acetate, Cu₄(*m*₉-CBT)₄ displayed a peak at m/z 1088.26, corresponding to the Cs⁺ attached peak of the cluster. The experimental isotopic distributions of both clusters matched well with the calculated distributions (inset right).

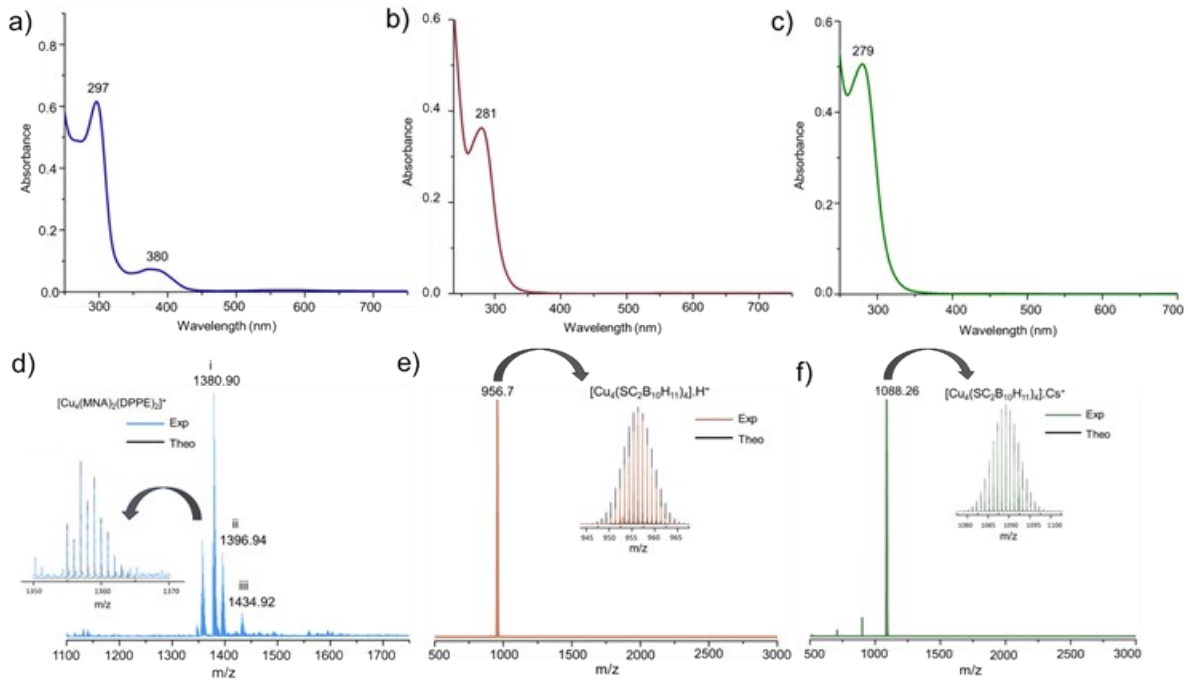


Fig S1 UV-vis absorption spectra of (a) $\text{Cu}_4(\text{MNA})_2(\text{DPPE})_2$, (b) $\text{Cu}_4(o_9\text{-CBT})_4$ and (c) $\text{Cu}_4(m_9\text{-CBT})_4$. ESI-MS spectra validate molecular integrity of (d) $\text{Cu}_4(\text{MNA})_2(\text{DPPE})_2$, (e) $\text{Cu}_4(o_9\text{-CBT})_4$ (formic acid as ionization enhancer), and (f) $\text{Cu}_4(m_9\text{-CBT})_4$ (caesium acetate as ionization enhancer). Insets: Experimental isotopic distributions align with theoretical predictions.

4. MicroED sample preparation and data collection workflow

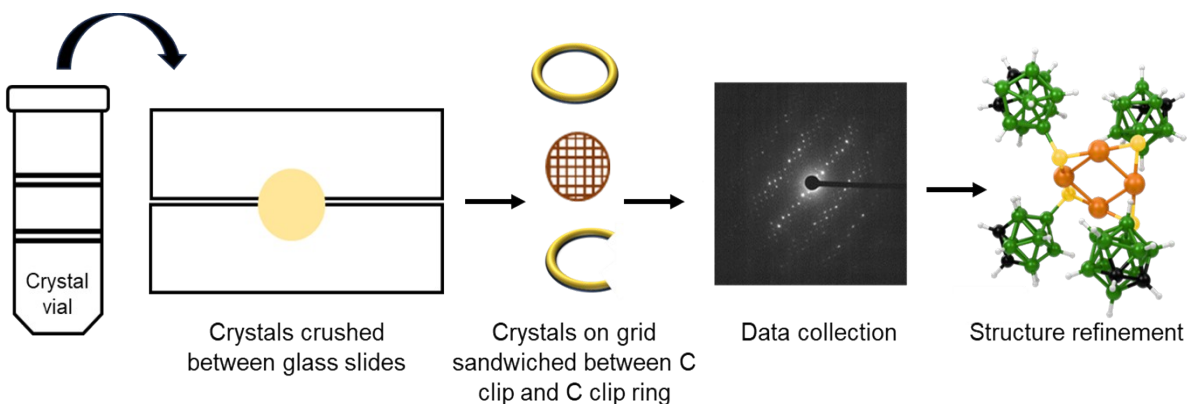


Fig. S2 Schematic workflow for MicroED structure determination: (1) Microcrystals are gently crushed to produce smaller crystallites; (2) these are deposited onto a lacey carbon TEM grid; (3) the grid is clipped and mounted in the cryo-EM; (4) electron diffraction data are collected from suitable crystallites; (5) data are processed and refined to yield the final atomic structure.

5. MicroED data acquisition workflow

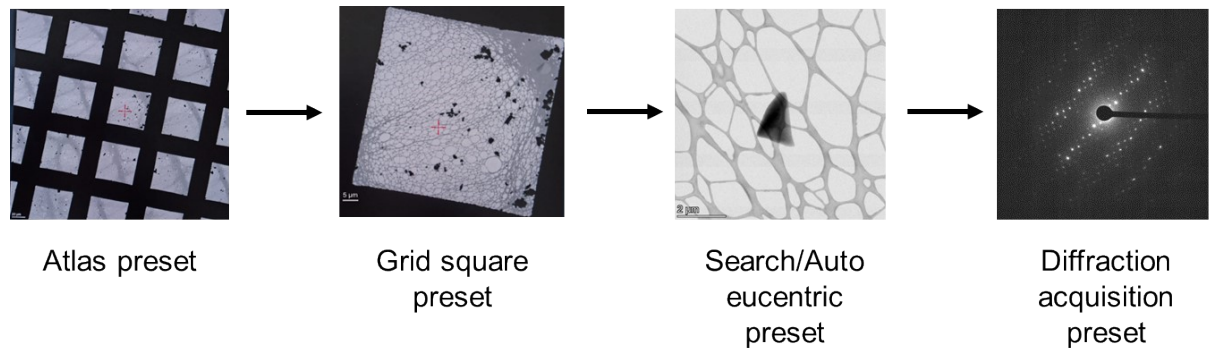


Fig. S3 Schematic workflow for continuous rotation MicroED data collection: Atlas preset (low-mag overview) → Grid square alignment → Auto-eucentric crystal centering → Diffraction preset for data acquisition, enabling atomic-resolution structure determination.

6. TEM tilt-series images

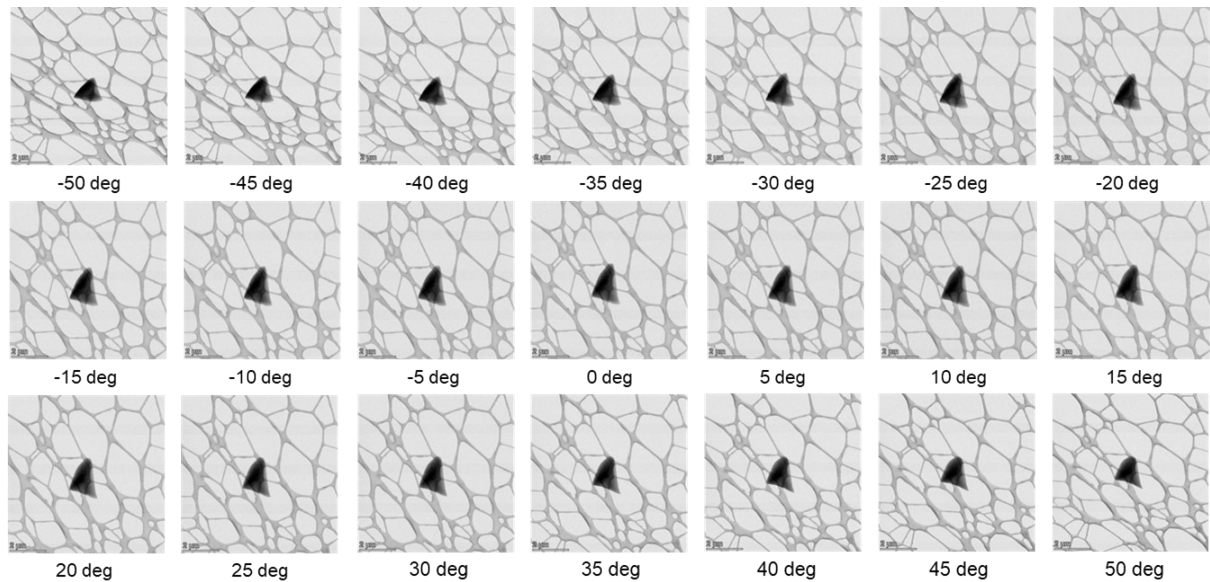


Fig. S4. Representative images of a Cu₄(MNA)₂(DPPE)₂ microcrystal captured at tilt angles from -50° to +50°.

Table S1. Structural comparison of Cu₄(MNA)₂(DPPE)₂ determined by SC-XRD and MicroED

Cu ₄ (MNA) ₂ (DPPE) ₂		
	SC-XRD	MicroED
Unit cell	a=19.2367(15) Å	a = 18.910(4) Å
	b=21.2522(17) Å	b = 21.160(4) Å
	c=14.6063(11) Å	c = 14.440(3) Å
	α = 90°	α = 90.0°
	β = 90°	β = 90.0°
	γ = 90°	γ = 90.0°
Space group	Pna2 ₁	Pna2 ₁
R1	0.0345	0.1372
wR2	0.0726	0.3296
GooF	1.077	0.866
Cu-Cu bond length	2.816 Å, 2.759 Å	2.743 Å, 2.729 Å
Cu-S bond length	2.836 Å, 2.295 Å, 2.249 Å, 2.937 Å, 2.337 Å, 2.211 Å	2.822 Å, 2.280 Å, 2.227 Å, 2.917 Å, 2.325 Å, 2.208 Å
Opposite S distance	4.161 Å	4.128 Å
Cu-S-Cu bond angle	74.64°, 76.59° 143.32°, 140.28° 71.89°, 73.34°	72.32°, 73.98° 143.06°, 139.42° 73.60°, 74.98°
Cu-P bond length	2.170 Å, 2.221 Å 2.212 Å, 2.181 Å	2.160 Å, 2.209 Å 2.205 Å, 2.193 Å
Cu-N bond length	2.016 Å, 2.026 Å	2.011 Å, 2.037 Å

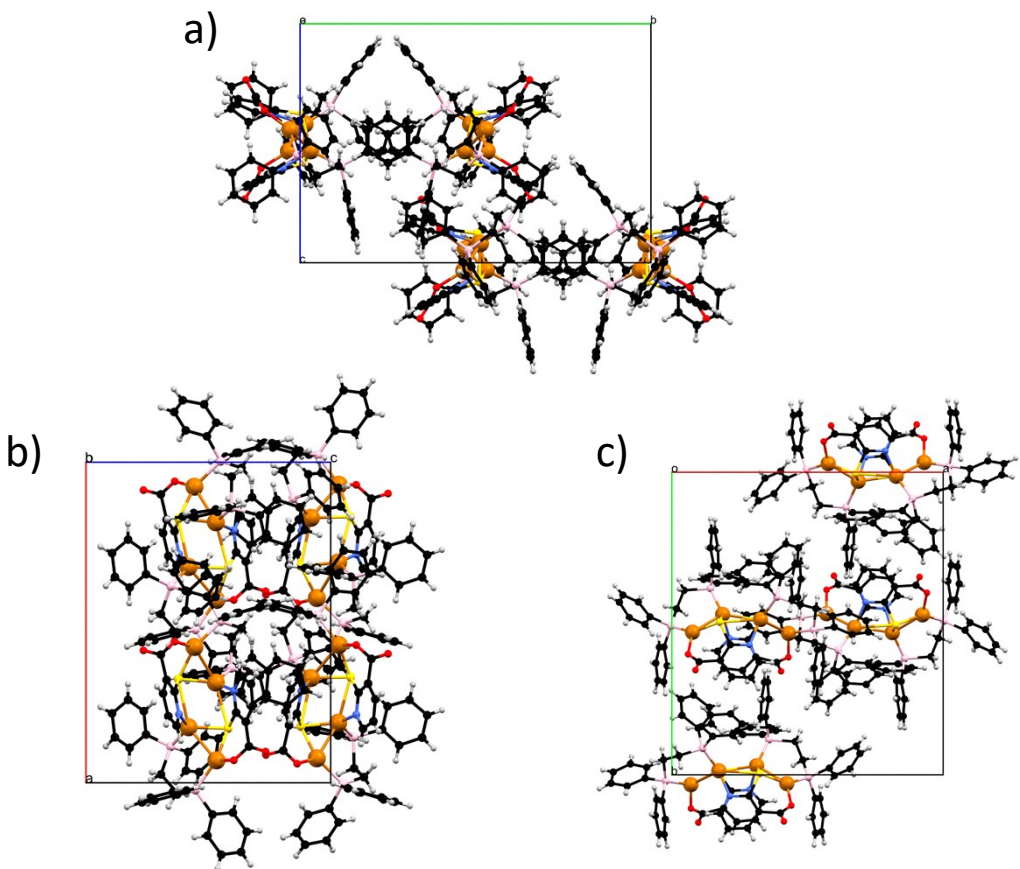


Fig. S5 Unit cell packing of $\text{Cu}_4(\text{MNA})_2(\text{DPPE})_2$ determined by MicroED along (a) a -axis, (b) b -axis, and (c) c -axis. Color code: Cu (orange), S (yellow), O (red), N (blue), P (pink), C (black), H (white).

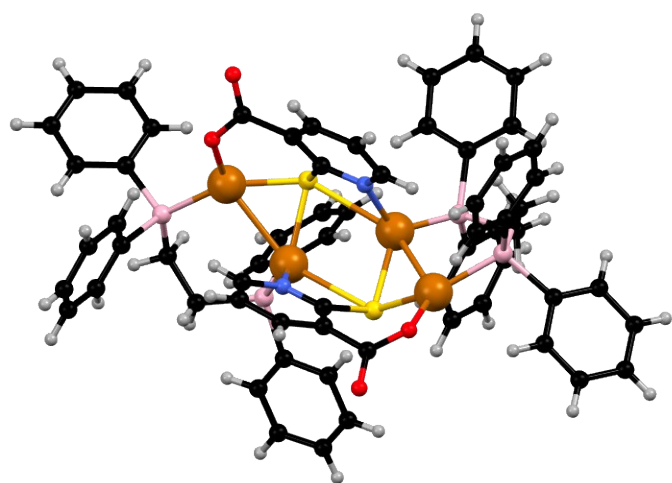


Fig. S6 Single-crystal X-ray structure of $\text{Cu}_4(\text{MNA})_2(\text{DPPE})_2$, illustrating the atomic arrangement and ligand coordination. Color code: Cu (orange), S (yellow), O (red), N (blue), P (pink), C (black), H (white).

Table S2. Structural comparison of Cu₄(m₉-CBT)₄ determined by SC-XRD and MicroED.

Cu ₄ (m ₉ -CBT) ₄		
	SC-XRD	MicroED
Unit cell	a = 11.3989(7) Å b = 11.9482(7) Å c = 32.3144(19) Å α = 90° β = 91.213(2)° γ = 90°	a = 12.250(2) Å b = 13.320(3) Å c = 16.050(3) Å α = 97.18(3)° β = 110.76(3)° γ = 99.99(3)°
Space group	P2 ₁ /c	P -1
R1	0.0986	0.1720
wR2	0.1819	0.4196
GooF	1.116	1.522
Cu-Cu bond length	2.682 Å, 2.705 Å 2.779 Å, 2.692 Å	2.673 Å, 2.775 Å 2.719 Å, 2.725 Å
Cu-Cu-Cu bond angle	89.91°, 89.75° 88.17°, 92.11°	89.72°, 89.83° 89.22°, 91.24°
Cu-S-Cu bond angle	76.48°, 77.29° 80.20°, 76.62°	79.59°, 76.55° 78.20°, 78.01°
Opposite S distance	5.415 Å, 5.495 Å	5.604 Å, 5.463 Å
Carborane B-S distance	1.86 Å, 1.86 Å 1.87 Å, 1.91 Å	1.86 Å, 1.86 Å, 1.86 Å, 1.90 Å

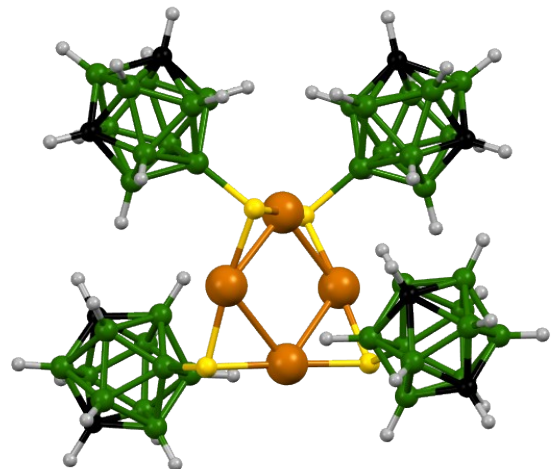


Fig. S7. Single-crystal X-ray structure of $\text{Cu}_4(\text{m}_9\text{-CBT})_4$, highlighting the square planar Cu_4 core and ligand coordination (toluene undetected in SC-XRD analysis). Color code: Cu (orange), S (yellow), B (green), C (black), H (white).

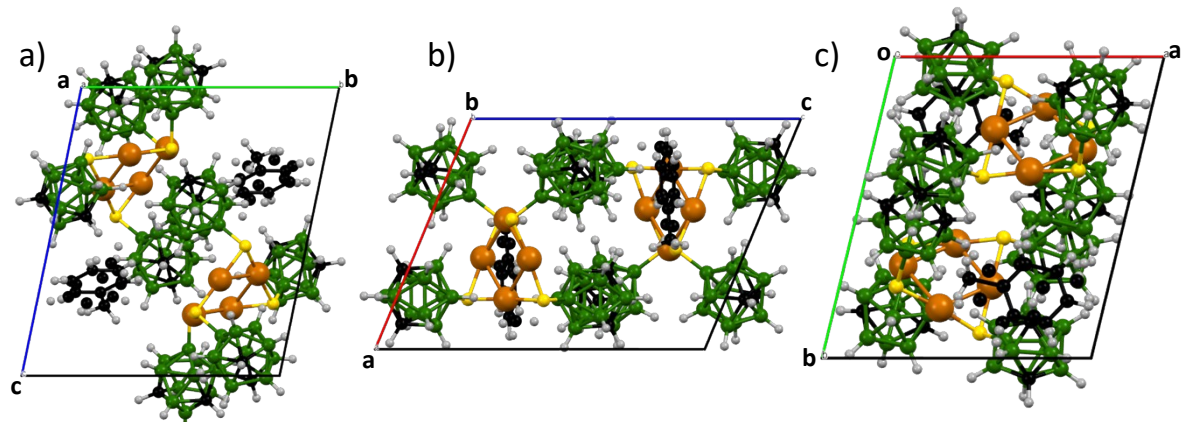


Fig. S8. MicroED-determined unit cell packing of $\text{Cu}_4(\text{m}_9\text{-CBT})_4$ along (a) a -axis, (b) b -axis, and (c) c -axis. Color code: Cu (orange), S (yellow), B (green), C (black), H (white).

Table S3. Structural comparison of Cu₄(o₉-CBT)₄ determined by SC-XRD and MicroED

	Cu ₄ (o ₉ -CBT) ₄		
	SC-XRD	MicroED	MicroED after solvent vapor exposure
Unit cell	a = 11.434(6) Å	a = 11.310(2) Å	a = 11.300(2) Å
	b = 11.434(6) Å	b = 11.310(2) Å	b = 11.300(2) Å
	c = 29.439(16) Å	c = 29.080(6) Å	c = 29.050(6) Å
	α = 90°	α = 90.0°	α = 90.0°
	β = 90°	β = 90.0°	β = 90.0°
	γ = 120°	γ = 120.0°	γ = 120.0°
Space group	P3 ₁ 21	P 3 ₂ 2 1	P 3 ₂ 2 1
R1	0.0513	0.1278	0.1271
wR2	0.1266	0.3409	0.3295
GooF	1.121	1.070	1.142
Cu-Cu bond length	2.684 Å, 2.684 Å	2.686 Å, 2.686 Å	2.667 Å, 2.667 Å
	2.728 Å, 2.728 Å	2.662 Å, 2.662 Å	2.698 Å, 2.698 Å
Cu-Cu-Cu bond angle	87.29°, 93.58°	85.48°, 94.04°	85.42°, 93.95°,
	85.54°, 93.58°	86.44°, 94.04°	86.67°, 93.95°
Cu-S-Cu bond angle	76.58°, 78.13°	76.99°, 76.99°	76.37°, 76.37°
	78.13°, 76.58°	75.78°, 75.78°	78.08°, 78.08°
Opposite S distance	5.540 Å, 5.540 Å	5.542 Å, 5.542 Å	5.503 Å, 5.503 Å
Carborane B-S distance	1.88 Å, 1.88 Å	1.85 Å, 1.85 Å	1.86 Å, 1.86 Å
	1.89 Å, 1.89 Å	1.88 Å, 1.88 Å	1.85 Å, 1.85 Å

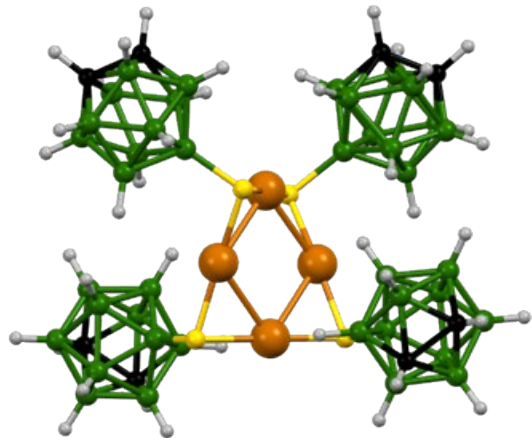


Fig. S9. Single crystal X-ray structure of $\text{Cu}_4(\text{o}_9\text{-CBT})_4$. Color code: Cu (orange), S (yellow), B (green), C (black), H (white).

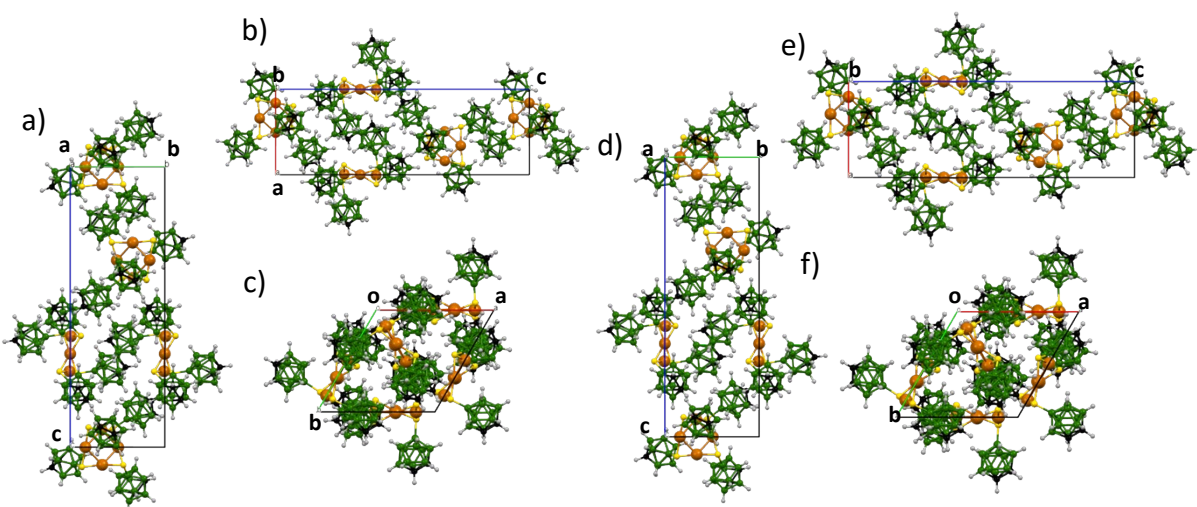


Fig. S10. MicroED analysis of $\text{Cu}_4(\text{o}_9\text{-CBT})_4$ unit cell packing. (a–c) Initial crystalline state and (d–f) post-solvent recrystallization viewed along a -, b -, and c -axes, respectively. Identical packing arrangements confirm structural restoration. Color code: Cu (orange), S (yellow), B (green), C (black), H (white).

Table S4. MicroED and SC-XRD - crystal data and structure refinement for Cu₄(MNA)₂(DPPE)₂

	MicroED	*SC-XRD
Empirical formula	C64 H54 Cu4 N2 O4 P4 S2	C64 H54 Cu4 N2 O4 P4 S2
Formula weight	1357.25	1357.25
Temperature	77(2) K	173(2) K
Crystal system	Orthorhombic	Orthorhombic
Space group	P n a 2 ₁	P n a 2 ₁
a (Å)	18.910(4) Å	19.2367(15) Å
b (Å)	21.160(4) Å	21.2522(17) Å
c (Å)	14.440(3) Å	14.6063(11) Å
α (°)	90°	90°
β (°)	90°	90°
γ (°)	90°	90°
V (Å ³)	5778(2) Å ³	5971.4(8) Å ³
Z	4	4
Density (cal. Mg/m ³)	1.560 Mg/m ³	1.510 Mg/m ³
Absorption coefficient	0.000 mm ⁻¹	1.632 mm ⁻¹
F(000)	1024	2768
Theta range for data collection	0.053 to 0.705°	3.064 to 28.301°
Index ranges	-23<=h<=23, -26<=k<=26, -18<=l<=18	-25<=h<=25, -28<=k<=28, -19<=l<=19
Reflections collected	46512	283464
Independent reflections	11692 [R(int) = 0.1825]	14836 [R(int) = 0.0908]
Completeness to theta	99.8 %	99.7 %
Extinction coefficient	1487(102)	n/a
Data / restraints / parameters	11692 / 733 / 722	14836 / 1 / 722
Goodness-of-fit on F ²	0.866	1.077
Final R indices [I>2sigma(I)]	R1 = 0.1372, wR2 = 0.3296	R1 = 0.0345, wR2 = 0.0726
R indices (all data)	R1 = 0.1587, wR2 = 0.3492	R1 = 0.0470, wR2 = 0.0783
Largest diff. peak and hole	0.264 and -0.186 e.Å ⁻³	0.770 and -0.391 e.Å ⁻³
CCDC No.	2391649	2339995

Table S5. MicroED and SC-XRD - crystal data and structure refinement for Cu₄(o₉-CBT)₄

	MicroED	MicroED after solvent vapor exposure	*SC-XRD
Empirical formula	C8 H44 B40 Cu4 S4	C8 H44 B40 Cu4 S4	C8 H44 B40 Cu4 S4
Formula weight	955.23	955.23	955.23
Temperature	77(2) K	77(2) K	296(2) K
Crystal system	Trigonal	Trigonal	Trigonal
Space group	P 3 ₂ 2 1	P 3 ₂ 2 1	P 3 ₁ 2 1
a (Å°)	11.310(2) Å	11.300(2) Å	11.4344(6) Å
b (Å°)	11.310(2) Å	11.300(2) Å	11.4344(6) Å
c (Å°)	29.080(6)	29.050(6) Å	29.4398(16) Å
α (°)	90.00	90.00	90.00
β (°)	90.00	90.00	90.00
γ (°)	120.00	120.00	120.00
V (Å°) ³	3221.4(13) Å ³	3212.4(13) Å ³	3333.4(4) Å ³
Z	3	3	3
Density (cal. Mg/m ³)	1.477 Mg/m ³	1.481 Mg/m ³	1.428 Mg/m ³
Absorption coefficient	0.000 mm ⁻¹	0.000 mm ⁻¹	2.091 mm ⁻¹
F(000)	594	594	1416
Theta range for data collection	0.058 to 0.627°	0.058 to 0.628°	2.922 to 26.057°
Index ranges	-9<=h<=10, -12<=k<=12, -32<=l<=32	-12<=h<=12, -12<=k<=12, -32<=l<=32	-14<=h<=13, -14<=k<=14, -36<=l<=36
Reflections collected	7717	19119	64165
Independent reflections	3080 [R(int) = 0.1500]	3088 [R(int) = 0.2564]	4384 [R(int) = 0.0563]
Completeness to theta	99.7 %	99.6 %	99.6 %
Extinction coefficient	505(72)	656(55)	n/a
Data / restraints / parameters	3080 / 584 / 255	3088 / 956 / 255	4384/0/255
Goodness-of-fit on F ²	1.070	1.142	1.121
Final R indices [I>2sigma(I)]	R1 = 0.1278, wR2 = 0.3409	R1 = 0.1271, wR2 = 0.3295	R1 = 0.0513, wR2 = 0.1266
R indices (all data)	R1 = 0.1890, wR2 = 0.3780	R1 = 0.1751, wR2 = 0.3598	R1 = 0.0570, wR2 = 0.1305
Largest diff. peak and hole	0.172 and -0.158 e.Å ⁻³	0.187 and -0.150 e.Å ⁻³	1.205 and -0.613 e.Å ⁻³
CCDC No.	2391700	2443461	2192348

Table S6. MicroED and SC-XRD - crystal data and structure refinement for Cu₄(m₉-CBT)₄

	MicroED	*SC-XRD
Empirical formula	C15 H52 B40 Cu4 S4	C15 H52 B40 Cu4 S4
Formula weight	1047.37	955.23
Temperature	77	296(2)
Crystal system	Triclinic	Monoclinic
Space group	P -1	P2 ₁ /c
a (Å°)	12.250(2) Å	11.3989(7) Å
b (Å°)	13.320(3) Å	11.9482(7) Å
c (Å°)	16.050(3) Å	32.3144(19) Å
α (°)	97.18(3)°	90°
β (°)	110.76(3)°	91.213(2)°
γ (°)	99.99(3)°	90°
V (Å°) ³	2361.7(9) Å ³	4400.1(5) Å ³
Z	2	4
Density (cal. Mg/m ³)	1.473 Mg/m ³	1.442 Mg/m ³
Absorption coefficient	0.000 mm ⁻¹	2.112 mm ⁻¹
F(000)	440	1888
Theta range for data collection	0.038 to 0.626°	3.044 to 23.439°
Index ranges	-13<=h<=13, -14<=k<=14, -17<=l<=17	-12<=h<=12, -13<=k<=13, -36<=l<=36
Reflections collected	23335	54022
Independent reflections	6189 [R(int) = 0.2364]	6415 [R(int) = 0.1819]
Completeness to theta	91.2 %	99.2 %
Extinction coefficient	3093(18)	n/a
Data / restraints / parameters	6189 / 1542 / 657	6415/298/505
Goodness-of-fit on F ²	1.522	1.116
Final R indices [I>2sigma(I)]	R1 = 0.1720, wR2 = 0.4196	R1 = 0.0986, wR2 = 0.1819
R indices (all data)	R1 = 0.2457, wR2 = 0.4590	R1 = 0.1808, wR2 = 0.2141
Largest diff. peak and hole	0.344 and -0.234 e.Å ⁻³	0.484 and -0.429 e.Å ⁻³
CCDC No.	2391697	2192353

Table S7. Atomic coordinates ($\times 10^4$) and equivalent isotropic displacement parameters ($\text{\AA}^2 \times 10^3$) for **MicroED structure of Cu₄(MNA)₂(DPPE)₂**. U(eq) is defined as one third of the trace of the orthogonalized U^{ij} tensor.

	x	y	z	U(eq)
Cu(1)	4299(2)	5325(3)	5331(3)	29(1)
Cu(2)	3268(2)	4866(2)	4193(3)	24(1)
Cu(3)	1873(2)	4700(2)	5306(3)	24(1)
Cu(4)	763(2)	5287(3)	4434(3)	27(1)
C(1)	3865(7)	6286(8)	6661(11)	25(3)
C(2)	3094(7)	6107(8)	6526(10)	22(3)
C(3)	2606(7)	6551(8)	6820(11)	29(3)
C(4)	1916(8)	6484(9)	6744(12)	36(4)
C(5)	1685(7)	5916(8)	6317(12)	32(4)
C(6)	2812(7)	5536(7)	6137(10)	23(3)
C(7)	1003(8)	6265(9)	3060(11)	31(4)
C(8)	1792(7)	6221(8)	3295(12)	30(3)
C(9)	2211(8)	6764(8)	3151(13)	36(4)
C(10)	2924(9)	6786(9)	3366(15)	49(5)
C(11)	3215(7)	6275(8)	3700(10)	27(3)
C(12)	2154(7)	5703(7)	3617(10)	22(3)
C(13)	5364(9)	5864(8)	3731(11)	31(3)
C(14)	5242(8)	6469(8)	4109(11)	34(4)
C(15)	5281(10)	6972(9)	3553(11)	40(4)
C(16)	5462(8)	6956(8)	2635(11)	31(3)
C(17)	5610(9)	6346(8)	2288(11)	32(3)
C(18)	5556(9)	5823(9)	2798(11)	36(4)
C(19)	5987(7)	5118(8)	5170(11)	28(3)
C(20)	6648(7)	5372(9)	4966(14)	38(4)
C(21)	7243(8)	5282(9)	5528(12)	41(4)
C(22)	7160(10)	4909(11)	6338(15)	53(5)
C(23)	6527(9)	4643(9)	6570(11)	40(4)
C(24)	5928(10)	4755(9)	6001(12)	40(4)
C(25)	5308(7)	4505(8)	3722(10)	27(3)
C(26)	4738(7)	4371(7)	3065(10)	23(3)
C(27)	4038(6)	3453(7)	4170(10)	21(3)

C(28)	4624(8)	3037(8)	4084(13)	40(4)
C(29)	4666(9)	2499(10)	4622(12)	43(5)
C(30)	4199(8)	2368(8)	5304(12)	38(4)
C(31)	3619(7)	2768(8)	5412(11)	31(3)
C(32)	3548(8)	3315(8)	4858(10)	31(4)
C(33)	3495(8)	3728(7)	2454(9)	21(3)
C(34)	3909(8)	3407(9)	1786(11)	36(4)
C(35)	3581(9)	3028(9)	1184(12)	41(4)
C(36)	2836(9)	2986(8)	1068(12)	39(4)
C(37)	2415(8)	3320(9)	1722(12)	35(4)
C(38)	2765(8)	3685(8)	2366(11)	32(4)
C(39)	1548(8)	3090(7)	5375(10)	27(3)
C(40)	1715(9)	3109(9)	4436(12)	40(4)
C(41)	1700(10)	2516(10)	3955(13)	51(5)
C(42)	1586(9)	1944(9)	4402(11)	39(4)
C(43)	1473(8)	1937(9)	5303(11)	35(3)
C(44)	1424(10)	2500(8)	5820(11)	41(4)
C(45)	1663(8)	3667(9)	7102(10)	29(3)
C(46)	2386(9)	3671(10)	7320(13)	42(5)
C(47)	2585(10)	3552(9)	8219(11)	38(4)
C(48)	2109(10)	3435(10)	8941(14)	48(5)
C(49)	1407(10)	3438(9)	8733(12)	44(4)
C(50)	1170(8)	3542(8)	7796(10)	28(3)
C(51)	450(7)	3904(7)	5953(10)	22(3)
C(52)	175(7)	4515(8)	6356(10)	25(3)
C(53)	-807(9)	4779(9)	4943(12)	39(4)
C(54)	-1234(6)	4290(7)	5319(12)	28(3)
C(55)	-1804(7)	4058(9)	4826(12)	34(4)
C(56)	-1932(9)	4298(9)	3953(11)	39(4)
C(57)	-1566(9)	4805(10)	3605(13)	47(5)
C(58)	-992(7)	5028(8)	4078(10)	27(3)
C(59)	-291(7)	5778(7)	6145(10)	22(3)
C(60)	-460(10)	5784(10)	7073(12)	45(4)
C(61)	-592(12)	6310(11)	7611(12)	53(5)
C(62)	-517(9)	6882(10)	7161(12)	42(4)
C(63)	-301(8)	6928(9)	6234(12)	37(4)
C(64)	-174(10)	6396(8)	5702(12)	41(4)
N(1)	2124(6)	5488(7)	6046(9)	23(2)

N(2)	2863(6)	5704(6)	3807(8)	19(2)
O(1)	4297(6)	6114(7)	6042(10)	32(3)
O(2)	4025(6)	6579(7)	7341(9)	31(3)
O(3)	596(6)	6015(8)	3627(10)	40(4)
O(4)	870(7)	6541(7)	2351(9)	32(3)
S(1)	3300(3)	4890(4)	5802(5)	22(2)
S(2)	1761(4)	4951(4)	3778(5)	25(2)
P(1)	5224(4)	5204(4)	4472(6)	26(2)
P(2)	-33(4)	5085(4)	5497(5)	23(2)
P(3)	3869(4)	4123(4)	3463(5)	22(2)
P(4)	1423(4)	3839(4)	5934(5)	25(2)

Table S8. Atomic coordinates ($\times 10^4$) and equivalent isotropic displacement parameters ($\text{\AA}^2 \times 10^3$) for **MicroED structure of Cu₄(o₉-CBT)₄ before grinding** U(eq) is defined as one third of the trace of the orthogonalized U^{ij} tensor.

	x	y	z	U(eq)
Cu(1)	10078(6)	6686(7)	3960(2)	39(1)
Cu(2)	10000	4932(8)	3333	41(2)
Cu(3)	10000	8391(8)	3333	37(2)
C(1)	8337(19)	1409(19)	4982(5)	48(4)
C(2)	9160(20)	1240(20)	4533(6)	58(4)
C(3)	4160(20)	5330(20)	3811(6)	65(4)
C(4)	4900(20)	6840(20)	4056(7)	73(5)
B(1)	10060(19)	4010(20)	4337(6)	35(4)
B(2)	9130(20)	2310(20)	4111(6)	43(4)
B(3)	10580(20)	2790(20)	4457(7)	57(4)
B(4)	10000(20)	2090(20)	5013(7)	61(5)
B(5)	10580(20)	3790(20)	4898(6)	57(4)
B(6)	9170(20)	2930(20)	5252(6)	59(5)
B(7)	7810(20)	2510(20)	4885(5)	42(4)
B(8)	9230(20)	4100(20)	4829(6)	50(4)
B(9)	8280(20)	3100(20)	4355(6)	38(4)
B(10)	7690(20)	1420(20)	4462(6)	41(4)
B(11)	7400(20)	7020(20)	3940(6)	40(4)
B(12)	6660(20)	6740(20)	3394(6)	46(4)
B(13)	6390(20)	7770(30)	3800(7)	61(4)
B(14)	6300(30)	7090(30)	4347(7)	63(5)
B(15)	6390(20)	5600(20)	4275(6)	43(4)
B(16)	6560(20)	5350(20)	3679(5)	40(4)
B(17)	4860(20)	4390(20)	3945(6)	50(4)
B(18)	4750(20)	5490(30)	4348(8)	64(5)
B(19)	5080(30)	6690(30)	3501(7)	66(5)
B(20)	5080(30)	5140(30)	3386(7)	61(5)
S(1)	11130(9)	5517(10)	3970(3)	43(2)
S(2)	9294(9)	8060(9)	4038(2)	42(2)

Table S9. Atomic coordinates ($\times 10^4$) and equivalent isotropic displacement parameters ($\text{\AA}^2 \times 10^3$) for **MicroED structure of Cu₄(o₉-CBT)₄ after solvent vapour exposure**. U(eq) is defined as one third of the trace of the orthogonalized U^{ij} tensor.

	x	y	z	U(eq)
Cu(1)	8394(6)	10000	6667	37(2)
Cu(2)	6671(6)	10063(5)	6037(2)	45(1)
Cu(3)	4923(7)	10000	6667	44(2)
B(1)	7009(18)	7408(16)	6066(7)	40(3)
B(2)	5526(17)	6353(17)	5715(7)	44(4)
B(3)	5334(18)	6503(17)	6319(7)	43(3)
B(4)	6761(17)	6665(17)	6614(7)	41(3)
B(5)	7856(18)	6499(18)	6224(7)	47(4)
B(6)	7078(19)	6318(19)	5664(8)	51(4)
B(7)	5531(18)	4790(18)	5638(8)	54(4)
B(8)	4457(19)	4918(17)	6051(7)	45(4)
B(9)	5135(19)	5071(18)	6606(7)	48(4)
B(10)	6678(18)	5135(17)	6530(8)	51(4)
B(11)	4005(17)	10101(17)	5657(7)	41(3)
B(12)	3850(19)	10632(19)	5109(7)	55(4)
B(13)	2707(18)	10490(20)	5572(7)	53(4)
B(14)	2298(18)	9100(19)	5899(8)	51(4)
B(15)	3102(15)	8280(17)	5637(6)	40(3)
B(16)	2454(19)	7794(19)	5100(7)	49(4)
B(17)	1377(17)	7661(18)	5540(7)	46(4)
B(18)	2070(20)	10010(20)	5011(8)	66(4)
B(19)	2840(20)	9160(20)	4756(8)	60(4)
B(20)	4039(19)	9180(20)	5163(7)	51(4)
C(1)	5324(16)	4110(14)	6188(7)	54(4)
C(2)	6841(17)	4858(17)	5957(7)	64(4)
C(3)	1364(17)	8321(17)	5022(7)	55(4)
C(4)	1204(17)	9114(17)	5483(7)	58(4)
S(1)	8023(7)	9283(6)	5963(3)	37(2)
S(2)	5509(8)	11119(8)	6033(3)	49(2)

Table S10. Atomic coordinates ($\times 10^4$) and equivalent isotropic displacement parameters ($\text{\AA}^2 \times 10^3$) for **MicroED structure of Cu₄(m₉-CBT)₄**. U(eq) is defined as one third of the trace of the orthogonalized U_{ij}^{ij} tensor.

	x	y	z	U(eq)
Cu(1)	5633(3)	7585(4)	7663(2)	46(1)
Cu(2)	3957(3)	6191(3)	7887(2)	41(1)
Cu(3)	3917(3)	8333(3)	6471(2)	43(1)
Cu(4)	2180(3)	6921(4)	6666(2)	46(1)
B(1)	6692(11)	6271(12)	9095(8)	43(3)
B(2)	7350(14)	7469(14)	9778(9)	72(3)
B(3)	8254(11)	6703(15)	9456(9)	71(3)
B(4)	7693(12)	5443(14)	9496(8)	57(3)
B(5)	6480(12)	5378(14)	9831(9)	53(3)
B(6)	6280(13)	6704(15)	9996(9)	66(3)
B(7)	8817(15)	7425(17)	10573(10)	80(3)
B(8)	8980(12)	6189(17)	10407(10)	79(4)
B(9)	6976(12)	6066(14)	10906(9)	66(3)
B(10)	8540(13)	6638(15)	11268(9)	69(3)
B(11)	2295(10)	7425(12)	8616(8)	38(2)
B(12)	1032(10)	7949(12)	8478(8)	46(3)
B(13)	2271(11)	8663(12)	8338(8)	49(3)
B(14)	3581(10)	8529(13)	9187(9)	51(3)
B(15)	3103(11)	7623(13)	9814(8)	55(3)
B(16)	1529(11)	7299(13)	9343(8)	48(3)
B(17)	1510(11)	9322(12)	8930(8)	48(3)
B(18)	3088(12)	9605(15)	9394(9)	59(3)
B(19)	2300(13)	8218(13)	10349(9)	60(3)
B(20)	2285(12)	9496(13)	10083(9)	58(3)
B(21)	2184(10)	6431(11)	4766(7)	35(2)
B(22)	2190(11)	5220(11)	5087(9)	44(3)
B(23)	933(10)	5415(12)	4201(9)	45(3)
B(24)	1413(12)	4310(14)	4056(9)	52(3)
B(25)	2989(12)	4638(13)	4529(9)	56(3)
B(26)	3451(10)	5896(12)	4949(9)	48(3)
B(27)	3004(11)	6529(13)	4046(8)	46(2)
B(28)	1427(11)	6253(12)	3577(8)	46(3)

B(29)	2153(11)	4361(13)	3310(9)	51(3)
B(30)	2207(12)	5640(13)	3055(9)	57(3)
B(31)	6642(10)	9426(12)	6881(8)	46(3)
B(32)	7251(13)	8408(16)	6457(9)	66(3)
B(33)	8202(12)	9423(15)	7377(9)	68(4)
B(34)	7729(11)	10607(14)	7131(9)	57(3)
B(35)	6464(11)	10236(14)	6115(9)	55(3)
B(36)	6192(12)	8966(14)	5704(9)	61(3)
B(37)	8668(13)	8972(16)	6494(11)	75(4)
B(38)	8948(12)	10346(15)	6909(9)	68(3)
B(39)	6975(12)	9765(14)	5273(9)	61(3)
B(40)	8484(12)	9849(13)	5753(9)	56(3)
C(1)	7607(13)	7347(13)	10844(8)	72(3)
C(2)	7831(10)	5438(12)	10569(7)	57(3)
C(3)	1101(9)	8444(11)	9520(7)	49(3)
C(4)	3475(10)	8946(13)	10184(7)	65(3)
C(5)	3356(10)	5409(12)	3920(8)	57(3)
C(6)	1040(10)	4934(11)	3217(8)	53(3)
C(7)	7436(11)	8785(12)	5524(8)	60(3)
C(8)	7870(10)	10682(12)	6164(8)	54(2)
S(1)	5666(4)	6017(5)	7865(3)	44(2)
S(2)	2165(4)	6231(5)	7816(3)	41(1)
S(3)	2116(4)	7628(5)	5509(3)	39(1)
S(4)	5637(4)	9169(5)	7507(3)	44(1)
C(9)	6099(10)	7614(16)	2890(11)	67(5)
C(10)	6703(15)	6885(13)	3264(14)	67(6)
C(11)	7951(15)	7129(14)	3647(12)	74(6)
C(12)	8595(10)	8102(16)	3657(12)	75(6)
C(13)	7990(15)	8831(13)	3283(15)	72(5)
C(14)	6742(15)	8587(15)	2899(13)	69(5)
C(15)	4757(15)	7360(20)	2428(16)	68(6)
C(9')	7573(13)	7651(17)	3393(12)	48(5)
C(10')	6530(17)	6889(14)	3177(16)	55(7)
C(11')	5415(13)	7096(15)	2738(15)	63(6)
C(12')	5344(13)	8064(17)	2515(11)	45(5)
C(13')	6388(17)	8826(14)	2731(16)	62(6)
C(14')	7502(14)	8620(15)	3170(15)	54(6)
C(15')	8775(19)	7440(30)	3901(18)	56(7)

References:

- 1 J. Plešek and S. Heřmánek, *Collect. Czechoslov. Chem. Commun.*, 1981, **46**, 687–692.
- 2 J. Plešek, Z. Janoušek and S. Heřmánek, *Collect. Czechoslov. Chem. Commun.*, 1978, **43**, 1332–1338.
- 3 S. Duary, A. Jana, A. Das, S. Acharya, A. R. Kini, J. Roy, A. K. Poonia, D. K. Patel, V. Yadav, P. K. S. Antharjanam, B. Pathak, A. Kumaran Nair Valsala Devi and T. Pradeep, *Inorg. Chem.*, 2024, **63**, 18727–18737.
- 4 A. Jana, M. Jash, W. Ahmed Dar, J. Roy, P. Chakraborty, G. Paramasivam, S. Lebedkin, K. Kirakci, S. Manna, S. Antharjanam, J. Machacek, M. Kucerakova, S. Ghosh, K. Lang, M. M. Kappes, T. Base and T. Pradeep, *Chem. Sci.*, 2023, **14**, 1613–1626.
- 5 J. Li, H. Z. Ma, G. E. Reid, A. J. Edwards, Y. Hong, J. M. White, R. J. Mulder and R. A. J. O’Hair, *Chem. Wein. Bergstr. Ger.*, 2018, **24**, 2070–2074.